



Measurement of Intra-Orbital Structures in Normal Chinese Adults Based on a Three-Dimensional Coordinate System

Yongrong Ji^{a,b}, Changxin Lai^c, Lixu Gu^c, and Xianqun Fan^{a,b}

^aDepartment of Ophthalmology, Ninth People's Hospital, Shanghai Jiao Tong University School of Medicine, Shanghai, China; ^bShanghai Key Laboratory of Orbital Diseases and Ocular Oncology, Shanghai, China; ^cSchool of Biomedical Engineering, Shanghai Jiao Tong University, Shanghai, China

ABSTRACT

Purpose of the study: This study was to establish a three-dimensional (3D) coordinate system and to study the normal dimensions of intra-orbital structures in Chinese adults.

Materials and methods: One hundred and forty-five adult Chinese were selected from patients who had undergone cranio-facial computed tomography scans with diagnosis other than orbital or ocular abnormality. An orbital 3D coordinate system was built on the basis of the scans. Morphological variables of intra-orbital structures were measured in this coordinate system. Bilateral symmetry, sexual dimorphism, and correlations between variables were investigated.

Results: No evident laterality was found in bilateral intra-orbital structures. The distance from the center of the eyeball to the prechiasmatic groove, the length of the optic nerve, and the thickness of rectus extraocular muscles were larger in males than in females. No sex-related difference was observed in the anteroposterior diameter of the eyeball or the exophthalmometric value. The exophthalmometric value was found to be related to the anteroposterior diameter of the eyeball, whereas the y-coordinate of the center of the eyeball had no correlation with the anteroposterior diameter of the eyeball. The optic nerve length was closely correlated to the distance from the center of the eyeball to the prechiasmatic groove.

Conclusions: The 3D coordinate system and measurement method established in this study can be applied to the standardization of orbital morphometry. The measurements obtained from normal Chinese adults may provide reference values for the morphology of intra-orbital structures.

ARTICLE HISTORY

Received 7 June 2018
Revised 30 July 2018
Accepted 2 August 2018

KEYWORDS

Three-dimensional coordinate system; orbital morphometry; exophthalmometry; optic nerve length; thickness of extraocular muscles

Introduction

The presence of morphological change in orbit is considered an evocative sign and sometimes the only sign of orbital diseases, such as enophthalmos for orbital fracture and exophthalmos for intra-orbital tumor and thyroid eye disease.¹⁻³ With respect to orbital surgery, intra-orbital structure measurement is key factor for surgical planning and post-operative evaluation.⁴⁻⁶



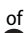
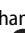
Cranio-facial computed tomography (CT) scans are common method of assessing the bony orbits and intra-orbital soft-tissue structures. Horizontal planes of the scan should be set parallel to Frankfort horizontal plane.⁷ The sagittal planes and coronal planes are reconstructed on the basis of the horizontal planes. However, in clinical practice, the scanning planes are not strictly adjusted according to the anatomical landmarks, so the reconstructed midsagittal plane cannot readily serve as the mirror plane of the head. In this way, the bilateral symmetry of orbits and intra-orbital structures cannot be evaluated directly on the scan image. Moreover, as the scanning planes may deviate from time to time, it is difficult to ascertain the exact displacement and morphological change of certain structures from two scans.

Currently, the diagnosis, evaluation, and planning of treatment of orbital diseases need more accurate medical imaging. The rough observations that can be made using original CT scans are not adequate for clinical applications such as in surgical navigation system and in quantified imaging evaluation. The aim of this study was to establish a three-dimensional (3D) coordinate system for orbital region and to study the normal measurements of intra-orbital structures in Chinese adults. The measurement method and data from this study may serve as the bases for subsequent studies on orbitopathy.

Materials and methods

Subjects

Subjects were selected from the adult patients (≥ 18 years old) who had undergone thin-slice cranio-facial CT scans with extension through the orbital region at Shanghai Ninth People's Hospital from 1st January 2016 to 1st January 2018 with electronic medical records indicating diagnoses other than orbital or ocular abnormality. The Medical Ethics Committee of Shanghai Ninth People's Hospital did not require informed consent for this retrospective study. The research adhered to the tenets of the Declaration of Helsinki.

CONTACT Xianqun Fan  fanxq@sjtu.edu.cn  Department of Ophthalmology, Shanghai Ninth People's Hospital, Shanghai Jiao Tong University School of Medicine, 639 Zhizaoju Road, Shanghai, 200011, China; Lixu Gu  gulixu@sjtu.edu.cn  School of Biomedical Engineering, Shanghai Jiao Tong University, 800 Dongchuan Road, Shanghai 200241, China

Color versions of one or more of the figures in the article can be found online at www.tandfonline.com/icey.

CT data acquisition

Cranio-facial CT scans of these subjects were collected from the hospital's CT database. Scans were obtained on a 64-row multi-slice CT (PHILIPS Brilliance) using high-resolution contiguous sections in an axial plane with the following protocol: slice thickness, 1.00 mm; field of view, 25×25 cm; matrix, 512×512 . All scan images used in the following reconstruction and analysis were in DICOM format.

Establishment of coordinate system and measurements of morphological variables

Image analysis was processed with SIMMED software (Shanghai Jiao Tong University, China). A 3D image of the skull was reconstructed on the basis of original CT scan. A 3D coordinate system was to be established for the skull. First, Frankfort plane was established by manually identifying the bony landmarks (right porion, left porion, and left orbitale) on the 3D skull. The horizontal planes were set parallel to the Frankfort plane. Midsagittal reference plane was set perpendicular to horizontal planes and passing through facial midline landmarks (nasion and prechiasmatic groove). The prechiasmatic groove is a bony midline landmark very close to optic chiasm, so it was set as the origin of the 3D coordinate system and also the endpoint of optic nerve (Figure 1). The Coronal planes and the coordinate axes were then automatically reformatted since the horizontal planes,

the sagittal planes, and the origin were fixed. The definitions of the anatomical landmarks, reference planes, coordinate axes, and morphological variables mentioned in this study are listed in Table 1. Each point in this 3D coordinate system had its x -axis, y -axis, and z -axis coordinates. All morphological variables were measured using software measuring tools (Figure 2).

Assessments of reproducibility

During the establishment of the coordinate system and the process of measurement, the bony landmarks and morphological variables were identified manually, so the reproducibility of this method needs to be assessed. In this study, 10 right orbits from 10 subjects were randomly selected for the assessment. For intraobserver variability, one observer, observer A, measured all the variables of these 10 orbits twice on different days. For interobserver variability, another observer, observer B, performed the same measurements independently on the same 10 orbits.

Statistical analysis

The statistical analysis was performed with Microsoft Office EXCEL 2007 (Microsoft, US) and SPSS 17.0 (SPSS, Chicago, IL, US). The measured values were presented as mean \pm SD. To assess reproducibility, the reliability analyses were performed

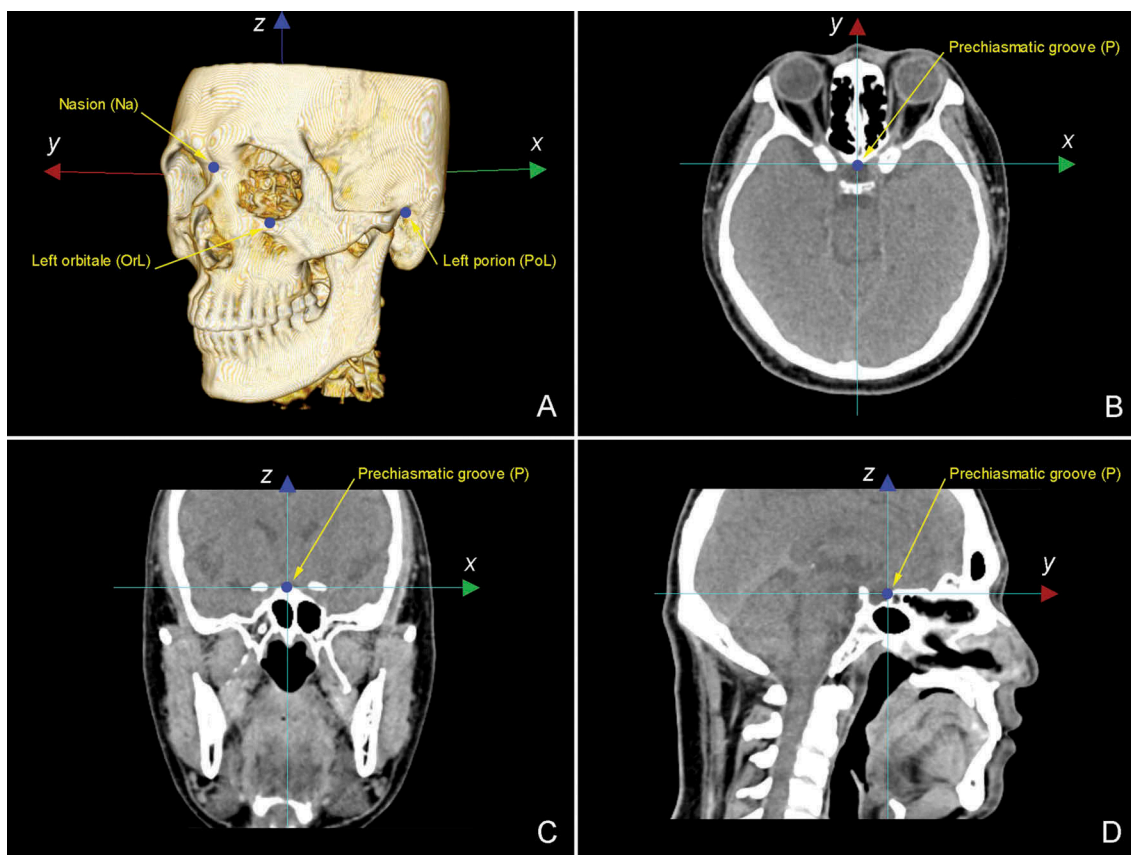
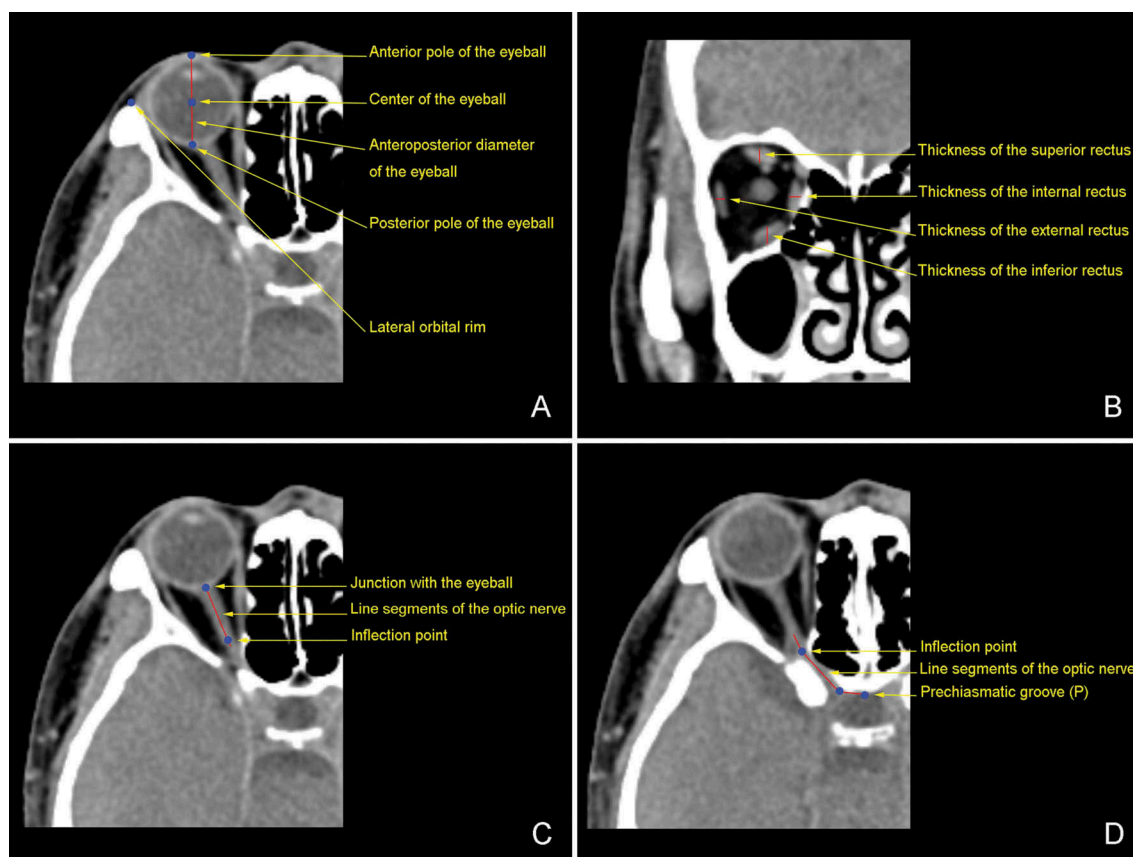


Figure 1. Anatomical landmarks, reference planes, and three-dimensional (3D) coordinate system.

- A. Anatomical landmarks and coordinate axes on reconstructed 3D skull: nasion (Na), left orbitale (OrL), left porion (PoL), x -axis, y -axis, and z -axis.
 B. Prechiasmatic groove (P, the origin of the 3D coordinate system), x -axis, and y -axis on horizontal reference plane (HRP).
 C. P, x -axis, and z -axis on coronal reference plane (CRP).
 D. P, y -axis, and z -axis on midsagittal reference plane (MRP).

Table 1. Definitions of anatomical landmarks, reference planes, 3D coordinate system, and morphological variables in this study.

Anatomical landmarks	Right porion (PoR)	Highest midpoint of roof of right external auditory meatus
	Left porion (PoL)	Highest midpoint of roof of left external auditory meatus
	Left orbitale (OrL)	Lowest point on left infraorbital margin of the orbit
	Nasion (Na)	Most posterior point on curvature between frontal bone and nasal bone
Reference planes	Prechiasmatic groove (P)	Vertical and transverse midpoint of prechiasmatic groove, set as the origin of the 3D coordinate system
	Frankfort horizontal plane	Passing through PoR, PoL, and OrL
	Horizontal reference plane (HRP)	Parallel to Frankfort horizontal plane, passing through P
	Midsagittal reference plane (MRP)	The left-right mirror plane of the head, perpendicular to HRP and passing through Na and P
3D coordinate system	Coronal reference plane (CRP)	Plane perpendicular to HRP and MRP, passing through P
	Origin	Prechiasmatic groove (P)
	x-axis (horizontal axis)	Intersecting line of HRP and CRP, from right to left when the head was in upright position
	y-axis (anteroposterior axis)	Intersecting line of HRP and MRP, from posterior to anterior and perpendicular to x-axis
Morphological variables	z-axis (vertical axis)	Intersecting line of MRP and CRP, from bottom to top and perpendicular to x-axis and y-axis
	Anteroposterior diameter of the eyeball	Anteroposterior coordinate value difference between the anterior and posterior pole of the eyeball
	Coordinates of the center of the eyeball	Coordinates of the midpoint between the anterior and posterior pole of the eyeball
	Exophthalmometric value	Anteroposterior coordinate value difference between the anterior pole of the eyeball and the lateral orbital rim
	Thickness of internal or external rectus	Largest horizontal diameter of the muscle in all coronal planes
	Thickness of superior or inferior rectus	Largest vertical diameter of the muscle in all coronal planes
	Optic nerve length	Length of the curve along the optic nerve from its junction with eyeball to the optic chiasm (taking P as the endpoint)

**Figure 2.** Measurements of morphological variables.

A. Locations of the landmarks on horizontal plane. The red line segment indicates the anteroposterior diameter of the eyeball. The exophthalmometric value is the anteroposterior coordinate value difference between the anterior pole of the eyeball and the lateral orbital rim on the same horizontal plane.

B. Thickness of rectus extraocular muscles (the largest horizontal diameter of the internal and external rectus muscles, the largest vertical diameter of the superior and inferior rectus muscles on coronal planes). Notably, the four muscles may be measured on different coronal planes.

C and D. The total length of the curved optic nerve was measured from its junction with eyeball to the optic chiasm (taking prechiasmatic groove as the endpoint) by adding up the lengths of the line segments between the inflection points drawn along the nerve which may pass through two or more neighboring horizontal planes.

and the intra-class correlation coefficients (ICCs) were calculated for all variables to determine the intra- and interobserver variability. The ICC was considered adequate if it was greater

than 0.75. The corresponding variables of bilateral orbits in the same subjects were compared using a paired samples *t*-test. Absolute *x*-axis coordinate value ($|x\text{-coordinate}|$) was used

to compare values between contralateral eyes directly. Comparisons between males and females were performed using an independent samples *t*-test. For correlation analysis between variables, a correlation coefficient over 0.5 indicated a strong correlation, and a coefficient less than 0.3 indicated a weak correlation. Regression formulas were fitted for those who had strong correlation. For all statistical analyses, a *P*-value less than 0.05 was considered statistically significant.

Results

A total of 290 orbits from 145 adult Chinese (75 men, 70 women), were included in this study. They ranged in age from 18 to 79 years with a median age of 51.

Repeated measurements of the variables by the same observer to test the intraobserver variability revealed the ICCs for all variables ranging from 0.961 to 0.985 ($P < 0.001$). Measurements by two observers to assess the interobserver variability revealed ICCs ranging from 0.926 to 0.971 ($P < 0.001$).

The measured values of bilateral variables are listed in Table 2. The variables showed no statistically significant difference between left and right sides ($P > 0.05$).

The variables for males and females are summarized in Table 3. The distance from the center of the eyeball to the prechiasmatic groove, the length of the optic nerve, and the thickness of rectus extraocular muscles presented significantly larger values in male than in female participants ($P < 0.05$). Anteroposterior diameter of the eyeball and

exophthalmometric value presented no significant difference between sexes ($P = 0.487$ and 0.439).

The optic nerve length was strongly correlated with the distance from the center of the eyeball to the prechiasmatic groove ($P < 0.001$, $r = 0.878$); a regression formula was therefore fitted (Table 4). The exophthalmometric value was correlated with the anteroposterior diameter of the eyeball ($P < 0.001$, $r = 0.321$), whereas the *y*-coordinate of the center of the eyeball had no correlation with the anteroposterior diameter of the eyeball ($P = 0.144$, $r = 0.086$).

Discussion

Morphology is an important concern in the diagnosis and evaluation of orbital diseases. The shape and size of bony orbits have been studied thoroughly because bony structures are easy to measure on preserved skulls and on radiologic images.^{8–10} However, intra-orbital structures rather than bony orbits are the most affected subjects in orbital diseases. Although many imaging techniques like echography, CT, and magnetic resonance imaging (MRI) scan are used in clinical practice to display intra-orbital structures, the measurements produced by different measurement methods differ from each other considerably and cannot be compared.^{11–13}

3D coordinate system is a standardized method of studying human anatomical morphology and has been used in cranial surgery to locate intra-cranial structures for more than 30 years.^{14,15} However, there is no standardized 3D coordinate system for orbits. So we set a 3D coordinate system specifically

Table 2. Comparison of measured values of bilateral variables ($n = 145$).

		Right (Mean ± SD)	Left (Mean ± SD)	R-L (Mean ± SD)	<i>t</i>	<i>P</i> *
Coordinates of the center of the eyeball (mm)	<i>x</i> -coordinate	30.95 ± 1.70	31.05 ± 1.73	−0.10 ± 0.96	−1.301	0.195
	<i>y</i> -coordinate	46.98 ± 3.34	47.04 ± 3.45	−0.06 ± 0.96	−0.800	0.425
	<i>z</i> -coordinate	−1.55 ± 1.98	−1.62 ± 1.99	0.07 ± 0.90	0.880	0.380
	$\sqrt{x^2 + y^2 + z^2}$ **	56.34 ± 3.21	56.46 ± 3.35	−0.12 ± 0.95	−1.467	0.144
Anteroposterior diameter of the eyeball (mm)		25.00 ± 1.86	24.91 ± 1.79	0.09 ± 0.78	1.386	0.168
Exophthalmometric value (mm)		16.24 ± 2.75	16.02 ± 2.78	0.22 ± 1.70	1.562	0.120
Thickness of rectus extraocular muscles (mm)	Superior rectus	3.22 ± 0.63	3.22 ± 0.61	0.01 ± 0.28	0.259	0.796
	Inferior rectus	4.35 ± 0.85	4.37 ± 0.81	−0.02 ± 0.66	−0.383	0.702
	Internal rectus	3.35 ± 0.59	3.37 ± 0.63	−0.01 ± 0.35	−0.412	0.681
	External rectus	4.38 ± 0.96	4.28 ± 1.02	0.09 ± 0.66	1.713	0.089
Optic nerve length (mm)		47.59 ± 3.69	47.36 ± 3.65	0.22 ± 1.61	1.675	0.096

*In a paired samples *t*-test, a *P*-value >0.05 indicates that the values of both sides were not significantly different.

** $\sqrt{x^2 + y^2 + z^2}$ indicates the distance from the center of the eyeball to the prechiasmatic groove (the origin of the coordinate system).

Table 3. Comparison of measured values between males and females.

		Male (75 subjects, 150 orbits) Mean ± SD	Female (70 subjects, 140 orbits) Mean ± SD	M-F difference Mean ± SE	Independent samples <i>t</i> -test for sex difference*
Coordinates of the center of the eyeball (mm)	<i>x</i> -coordinate	31.61 ± 1.67	30.34 ± 1.50	1.27 ± 0.19	$t = 6.765, P < 0.001$
	<i>y</i> -coordinate	48.22 ± 3.27	45.71 ± 3.03	2.51 ± 0.37	$t = 6.774, P < 0.001$
	<i>z</i> -coordinate	−2.22 ± 2.15	−0.90 ± 1.53	−1.31 ± 0.22	$t = −6.028, P < 0.001$
	$\sqrt{x^2 + y^2 + z^2}$ **	57.77 ± 3.07	54.92 ± 2.83	2.85 ± 0.35	$t = 8.203, P < 0.001$
Anteroposterior diameter of the eyeball (mm)		25.03 ± 1.33	24.88 ± 2.24	0.15 ± 0.22	$t = 0.696, P = 0.487$
Exophthalmometric value (mm)		16.25 ± 2.58	16.00 ± 2.96	0.25 ± 0.33	$t = 0.776, P = 0.439$
Thickness of rectus extraocular muscles (mm)	Superior rectus	3.32 ± 0.61	3.11 ± 0.61	0.20 ± 0.07	$t = 2.832, P = 0.005$
	Inferior rectus	4.53 ± 0.85	4.17 ± 0.76	0.36 ± 0.09	$t = 3.826, P < 0.001$
	Internal rectus	3.46 ± 0.62	3.25 ± 0.59	0.22 ± 0.07	$t = 3.042, P = 0.003$
	External rectus	4.47 ± 1.05	4.18 ± 0.89	0.30 ± 0.11	$t = 2.612, P = 0.009$
Optic nerve length (mm)		48.86 ± 3.49	45.99 ± 3.25	2.87 ± 0.40	$t = 7.220, P < 0.001$

*In an independent samples *t*-test, a *P*-value <0.05 indicates that the values for male and female were significantly different.

** $\sqrt{x^2 + y^2 + z^2}$ indicates the distance from the center of the eyeball to the prechiasmatic groove (the origin of the coordinate system).

Table 4. Correlation between morphological variables.

Independent variable (x)	Dependent variable (y)	P*	r	Regression formula**
Distance from the center of the eyeball to the prechiasmatic groove	Optic nerve length	<0.001	0.878	$y = 0.983x - 7.988$
Anteroposterior diameter of the eyeball	Exophthalmometric value	<0.001	0.321	
Anteroposterior diameter of the eyeball	y-coordinate of the center of the eyeball	0.144	0.086	

*In correlation analysis, a *P*-value <0.05 indicates that the correlation between these two variables was significant.

**Regression formula is fitted for those who had strong correlation ($r > 0.5$).

for orbital region to investigate the morphology and localization of intra-orbital structures.

The establishment of the coordinate system and the measurement procedure were semi-automatic in this study. The bony landmarks and morphological variables were identified manually. Then, the reference planes and coordinate axes can be adjusted automatically according to the bony landmarks and the variables would be measured using software tools. This method demonstrated adequate reproducibility, which suggests that it is appropriate for comparing the measurements made using the same criteria.

According to the literature and our previous studies, bony orbits remain stable after the age 18 and normally present left-right symmetry in shape and size.¹⁶⁻¹⁸ In this study, the positions of eyeballs were generally symmetrical, and the variables of optic nerve and rectus extraocular muscles were similar between left and right sides. Our findings confirmed that intra-orbital soft tissues also follow the rule of bilateral symmetry. Besides, the results of our study also listed the standard deviation of the bilateral differences for each variable, which may provide a normal reference range of bilateral differences for each variable within the general rule of symmetry.

The bony orbits are larger in males than in females according to the results of previous studies.^{10,19,20} We here observed the differences between sexes existing also in the position of the eyeball, the length of the optic nerve, and the thickness of rectus extraocular muscles but not in the anteroposterior diameter of the eyeball and exophthalmometric value. The exophthalmometric values in this study were similar to those of previous reports,²¹⁻²³ but the values of anteroposterior diameter of the eyeball were larger than the values of ocular axial length in the literature.²⁴⁻²⁶ Anteroposterior diameter of the eyeball and ocular axial length are similar variables that represent the size of the eyeball, but the anteroposterior diameter of the eyeball was measured in reconstructed CT images strictly along the anteroposterior axis, regardless of the direction of gaze, so the results may differ from those of ocular axial length measured using optical biometry.

The exophthalmometric value is the most widely used variable to represent the relative position of the eyeball. However, it is a variable only on anteroposterior axis, and unable to reflect the eyeball location on the horizontal or vertical axes. Moreover, according to the literature and the results of this study, the exophthalmometric value was found to be influenced by eyeball size to a considerable extent.^{21,22} Thus, we prefer to

use the coordinates of the center of the eyeball to represent the position of the eyeball. Coordinates of the center of the eyeball were not influenced by the anteroposterior diameter of the eyeball or the direction of gaze. Eyeball displacement would be described in accurate coordinate change rather than roughly as enophthalmos or exophthalmos.

Extraocular muscles are important intra-orbital structures concerning strabismus and orbitopathies especially the thyroid eye disease, of which the extraocular muscle involvement is a main diagnostic criterion and a key factor for severity assessment.²⁷⁻³⁰ Echography, CT, and MRI scans are all used in clinical practice to display extraocular muscle. However, the measurements deviate considerably using different measurement methods and on different measuring planes. And no single plane is ideal for measuring the anatomical thickness of all extraocular muscles.³¹⁻³³ In this study, we took the coronal planes as the standardized planes to measure the four rectus extraocular muscles. Notably, the muscle thickness measured in the coronal plane is not the same as the anatomical thickness of the muscle because the coronal plane is not perpendicular to the longitudinal axis of any muscle. However, this method of measurement is highly reproducible and the measurements can be compared if made using the same criteria. The normal measurement values provided in this study may help indicate the deformation of extraocular muscle sensitively.

The optic nerve extends from the optic disc to the optic chiasm, traversing the intraocular, intra-orbital, intracanalicular, and intracranial regions.^{34,35} Orbital diseases such as trauma and intra-orbital space-occupying lesions may all affect the optic nerve. In addition to direct compression and severing, stretching can also cause optic neuropathy, and the elongation of the optic nerve can be viewed under imaging.^{36,37} In this way, the measurements of the optic nerve may have special importance in these cases. However, according to previous studies and clinical observations, even normal optic nerves may vary considerably in length among individuals.^{35,38} The results of this study confirmed this variation and attributed it to individual variation in eyeball position because the optic nerve length was found to be closely correlated with the coordinate position of the eyeball. In other words, the location of the eyeball strongly affected the optic nerve length. The regression formulae worked out in this study can thus facilitate the estimation of the length of the curved optic nerve by providing the location of the eyeball. This method of estimation may help further studies on neuropathy regarding elongation of optic nerve or the studies on the extent of neuroplasticity when subjected to eyeball displacement and stretching.

The limitations of this study are inherent to the study design and measurement method. As the subjects were limited to normal Chinese adults, the growth of orbit during childhood and the aging of orbit in senile people were not taken into consideration in this study. The original CT scans were retrospectively collected from the database, so some factors such as the direction of gaze and refractive status were not controlled. However, we used the coordinates of the center of the eyeball instead of the exophthalmometric value to represent the position of the eyeball to avoid the influence of the gaze direction. The coordinates of the center

of the eyeball were also here confirmed to be unaffected by the anteroposterior diameter of the eyeball which is related to the refractive status. The establishment of the coordinate system and the measurement procedure included some manual steps which may cause errors in measurement. However, there is currently no fully automatic orbital morphometric method, and the intraobserver and interobserver variability reported here showed satisfactory results. Intersessional repeatability was not assessed in this study as two scans of the same subject were not available in this retrospective data collection. We intend to assess the intersessional repeatability in subsequent long-term studies of orbital disease using the same method.

Conclusions

The present study established a 3D coordinate system and measurement method which can be applied to the standardization of orbital morphometry. Bilateral symmetry, sexual dimorphism, and correlations between variables of intra-orbital structures were confirmed by using this method. The measurements obtained from normal Chinese adults may provide reference values for the morphology of intra-orbital structures.

Acknowledgments

The authors thank Qian Xu, Heng Lin, Chaowei Wu, and Xuan Xu (Shanghai Jiao Tong University) for their great help in image processing.

Declaration of Interests

The authors report no conflicts of interest. The authors alone are responsible for the content and writing of the paper.

Funding

This work was supported by the National Natural Science Foundation of China (31600971, 31701046 and 81600766), the Science and Technology Commission of Shanghai (17DZ2260100) and the National Key Research and Development Program of China (2016YFC0106200).

References

- Choi SH, Kang DH, Gu JH. The correlation between the orbital volume ratio and enophthalmos in unoperated blowout fractures. *Arch Plast Surg*. 2016;43(6):518–22. doi:10.5999/aps.2016.43.6.518.
- Tsai CC, Kau HC, Kao SC, Hsu WM. Exophthalmos of patients with Graves' disease in Chinese of Taiwan. *Eye*. 2006;20(5):569–73. doi:10.1038/sj.eye.6701925.
- Fang ZJ, Zhang JY, He WM. CT features of exophthalmos in Chinese subjects with thyroid-associated ophthalmopathy. *Int J Ophthalmol*. 2013;6(2):146–49. doi:10.3980/j.issn.2222-3959.2013.02.07.
- Clauser L, Galìè M, Pagliaro F, Tieghi R. Posttraumatic enophthalmos: etiology, principles of reconstruction, and correction. *J Craniofac Surg*. 2008;19(2):351–59. doi:10.1097/SCS.0b013e3180534361.
- Takahashi Y, Kakizaki H. Horizontal eye position in thyroid eye disease: a retrospective comparison with normal individuals and changes after orbital decompression surgery. *PloS One*. 2014;9(12):e114220. doi:10.1371/journal.pone.0114220.
- Ramieri G, Spada MC, Bianchi SD, Berrone S. Dimensions and volumes of the orbit and orbital fat in posttraumatic enophthalmos. *Dentomaxillofac Radiol*. 2000;29(5):302–11. doi:10.1038/sj/dmfr/4600551.
- Lundström A, Lundström F. The Frankfort horizontal as a basis for cephalometric analysis. *Am J Orthod Dentofacial Orthop*. 1995;107:537–40.
- Deveci M, Oztürk S, Sengezer M, Pabuşcu Y. Measurement of orbital volume by a 3-dimensional software program: an experimental study. *J Oral Maxillofac Surg*. 2000;58:645–48.
- Acer N, Sahin B, Ergür H, Basaloglu H, Ceri NG. Stereological estimation of the orbital volume: a criterion standard study. *J Craniofac Surg*. 2009;20(3):921–25. doi:10.1097/SCS.0b013e3181a1686d.
- Ji Y, Qian Z, Dong Y, Zhou H, Fan X. Quantitative morphometry of the orbit in Chinese adults based on a three-dimensional reconstruction method. *J Anat*. 2010;217(5):501–06. doi:10.1111/j.1469-7580.2010.01286.x.
- Guyomarc'h P, Dutailly B, Couture C, Coqueugniot H. Anatomical placement of the human eyeball in the orbit—validation using CT scans of living adults and prediction for facial approximation. *J Forensic Sci*. 2012;57(5):1271–75. doi:10.1111/j.1556-4029.2012.02075.x.
- Dick AD, Nangia V, Atta H. Standardised echography in the differential diagnosis of extraocular muscle enlargement. *Eye*. 1992;6(Pt 6):610–17. doi:10.1038/eye.1992.132.
- Tian S, Nishida Y, Isberg B, Lennerstrand G. MRI measurements of normal extraocular muscles and other orbital structures. *Graefes Arch Clin Exp Ophthalmol*. 2000;238:393–404.
- Brown RA, Roberts TS, Osborn AG. Stereotactic frame and computer software for CT-directed neurosurgical localization. *Invest Radiol*. 1980;15:308–12.
- Roberts DW, Strohbehn JW, Hatch JF, Murray W, Kettenberger H. A frameless stereotaxic integration of computerized tomographic imaging and the operating microscope. *J Neurosurg*. 1986;65(4):545–49. doi:10.3171/jns.1986.65.4.0545.
- Bentley RP, Sgouros S, Natarajan K, Dover MS, Hockley AD. Normal changes in orbital volume during childhood. *J Neurosurg*. 2002;96(4):742–46. doi:10.3171/jns.2002.96.4.0742.
- Chau A, Fung K, Yip L, Yap M. Orbital development in Hong Kong Chinese subjects. *Ophthalmic Physiol Opt*. 2004;24(5):436–39. doi:10.1111/j.1475-1313.2004.00217.x.
- Ji Y, Ye F, Zhou H, Xie Q, Ge S, Fan X. Bony orbital maldevelopment after enucleation. *J Anat*. 2015;227(5):647–53. doi:10.1111/joa.12372.
- Pretorius E, Steyn M, Scholtz Y. Investigation into the usability of geometric morphometric analysis in assessment of sexual dimorphism. *Am J Phys Anthropol*. 2006;129(1):64–70. doi:10.1002/ajpa.20251.
- Furuta M. Measurement of orbital volume by computed tomography: especially on the growth of orbit. *Jpn J Ophthalmol*. 2001;45:600–06.
- Bilen H, Gullulu G, Akcay G. Exophthalmometric values in a normal Turkish population living in the northeastern part of Turkey. *Thyroid*. 2007;17(6):525–28. doi:10.1089/thy.2006.0279.
- Chan W, Madge SN, Senaratne T, Senanayake S, Edussuriya K, Selva D, Casson RJ. Exophthalmometric values and their biometric correlates: the Kandy eye study. *Clin Exp Ophthalmol*. 2009;37(5):496–502. doi:10.1111/j.1442-9071.2009.02087.x.
- Wu D, Liu X, Wu D, Di X, Guan H, Shan Z, Teng W. Normal values of hertel exophthalmometry in a Chinese Han population from Shenyang, Northeast China. *Sci Rep*. 2015;5:8526. doi:10.1038/srep08526.
- Yin G, Wang YX, Zheng ZY, Yang H, Xu L, Jonas JB. Beijing eye study group. Ocular axial length and its associations in Chinese: the Beijing eye study. *PloS One*. 2012;7(8):e43172. doi:10.1371/journal.pone.0043172.
- Nangia V, Jonas JB, Sinha A, Matin A, Kulkarni M, Panda-Jonas S. Ocular axial length and its associations in an adult population of central rural India: the central India eye and medical study. *Ophthalmology*. 2010;117(7):1360–66. doi:10.1016/j.ophtha.2009.11.040.
- Wong TY, Foster PJ, Ng TP, Tielsch JM, Johnson GJ, Seah SK. Variations in ocular biometry in an adult Chinese population in Singapore: the Tanjong Pagar Survey. *Invest Ophthalmol Vis Sci*. 2001;42:73–80.

27. Bartalena L, Baldeschi L, Boboridis K, Eckstein A, Kahaly GJ, Marcocci C, Perros P, Salvi M, Wiersinga WM. European Group on Graves' Orbitopathy (EUGOGO). The 2016 European Thyroid Association/European Group on graves' orbitopathy guidelines for the management of graves' orbitopathy. *Eur Thyroid J*. 2016;5(1):9–26. doi:10.1159/000443828.
28. Xu L, Li L, Xie C, Guan M, Xue Y. Thickness of extraocular muscle and orbital fat in MRI predicts response to glucocorticoid therapy in Graves' ophthalmopathy. *Int J Endocrinol*. 2017;2017:3196059. doi:10.1155/2017/3196059.
29. Kvetny J, Puhakka KB, Røhl L. Magnetic resonance imaging determination of extraocular eye muscle volume in patients with thyroid-associated ophthalmopathy and proptosis. *Acta Ophthalmol Scand*. 2006;84(3):419–23. doi:10.1111/j.1600-0420.2005.00617.x.
30. Byun JS, Moon NJ, Lee JK. Quantitative analysis of orbital soft tissues on computed tomography to assess the activity of thyroid-associated orbitopathy. *Graefes Arch Clin Exp Ophthalmol*. 2017;255(2):413–20. doi:10.1007/s00417-016-3538-0.
31. Shen S, Fong KS, Wong HB, Looi A, Chan LL, Rootman J, Seah LL. Normative measurements of the Chinese extraocular musculature by high-field magnetic resonance imaging. *Invest Ophthalmol Vis Sci*. 2010;51(2):631–36. doi:10.1167/iovs.09-3614.
32. Demer JL, Kerman BM. Comparison of standardized echography with magnetic resonance imaging to measure extraocular muscle size. *Am J Ophthalmol*. 1994;118:351–61.
33. Lee JY, Bae K, Park KA, Lyu IJ, Oh SY. Correlation between extraocular muscle size measured by computed tomography and the vertical angle of deviation in thyroid eye disease. *PLoS One*. 2016;11(1):e0148167. doi:10.1371/journal.pone.0148167.
34. Unsöld R, Degroot J, Newton TH. Images of the optic nerve: anatomic-CT correlation. *AJR Am J Roentgenol*. 1980;135(4):767–73. doi:10.2214/ajr.135.4.767.
35. Bernstein SL, Meister M, Zhuo J, Gullapalli RP. Postnatal growth of the human optic nerve. *Eye*. 2016;30(10):1378–80. doi:10.1038/eye.2016.141.
36. Alvi A, Janecka IP, Kapadia S, Johnson BL, McVay W. Optic nerve elongation: does it exist? *Skull Base Surg*. 1996;6:171–80.
37. Peyster RG, Hoover ED, Hershey BL, Haskin ME. High-resolution CT of lesions of the optic nerve. *AJR Am J Roentgenol*. 1983;140(5):869–74. doi:10.2214/ajr.140.5.869.
38. Ettl A, Salomonowitz E, Koornneef L, Zonneveld FW. High-resolution MR imaging anatomy of the orbit. Correlation with comparative cryosectional anatomy. *Radiol Clin North Am*. 1998;36:1021–45.